Tectono-stratigraphic modelling of the Sardinian margin of the Tyrrhenian Sea

Spadini, G.; Bertotti, G.; Cloetingh, S.A.P.L.

published in
Tectonophysics
1995

DOI (link to publisher)
10.1016/0040-1951(95)00103-4

document version
Publisher's PDF, also known as Version of record

ELSEVIER

Tectonophysics 252 (1995) 269–284

TECTONOPHYSICS

Tectono-stratigraphic modelling of the Sardinian margin of the Tyrrhenian Sea

Giacomo Spadini *, Giovanni Bertotti, Sierd Cloetingh

Institute for Earth Sciences, Vrije Universiteit, De Boelelaan 1085, 1081 HV Amsterdam, Netherlands

Received 15 December 1994; accepted 3 April 1995

Abstract

Rifting of the east Sardinia passive margin was characterised by a southeastward migration of the site of extension through time. In the first stage of rifting (9–7 Ma), lithospheric thinning was mainly localised near Sardinia; crustal and subcrustal thinning factors averaged across the whole transect were 1.12 and 1.5, respectively. At 7 Ma, i.e. immediately before the onset of the Messinian salinity crisis, the basin floor was at depths of up to 1000 m in the west and less than few hundred metres in the east. During the second stage of rifting (between 7 and 5 Ma), the site of main extension was located in the central part of the future margin with average crustal and subcrustal thinning factors of 1.18 and 1.63, respectively. At 5 Ma, after the termination of the Messinian salinity crisis, the morphology of the basin floor had changed substantially with depths in general between 700 and 1000 m. Extension, during the last rifting stage before oceanic crust formation at 3.5 Ma, was mainly concentrated in the southeasternmost part of the profile; average crustal thinning factors increased dramatically to 1.95, while the subcrustal one remained almost unchanged (1.64). The analysis of temporal changes of thinning factors shows that the opening of the Tyrrhenian oceanic basin can be adequately explained with a depth-dependent pure-shear geometry with crustal and subcrustal thinning being accommodated on the same vertical column. Subcrustal thinning factors in the initial stages of rifting were higher than the crustal ones but the two become comparable approaching break-up. The regional compensation of changing loads coupled with a very deep depth of necking, is consistent with the observed subsidence trend and basin stratigraphy.

1. Introduction

The Tyrrhenian Sea oceanic basin (Fig. 1) developed superimposed on the Alpine–Apenninic belt. Late Tortonian extension between the Sardinian–Corsica block and the Adriatic (micro)plate started together with the counterclockwise rotation of the latter contemporaneous to a major change in the Africa–Europe pole of rotation (Dewey et al., 1989). Initially, extensional deformation was mainly localised along the border between the western parts of the chain and the adjacent Sardinian Paleozoic crust. Contemporaneous to rifting, thrusting was going on in the eastern part of the chain. This pattern remained constant through time with an eastward shift of the sites of maximum deformation. As a result, extensional structures progressively overprint contractional features, both younging towards the east (Patacca et al., 1990). The first oceanic crust, marking the end of the rifting stage, formed at 4.1 Ma (Sartori, 1990). The oldest sediments overlying the basalts of the Vavilov basin have been biostrati-

* Corresponding author.

SSDI 0040-1951(95)00103-4

graphically dated at about 3.5 Ma (Sartori, 1990). Continued rotation of the Adriatic plate caused further opening of the oceanic basins and the formation of a new spreading centre to the south (Marsili basin) with basalts less than 2 Ma old (Leg 107 Shipboard Party, 1986).

Spadini et al. (1995) have used a numerical model to constrain the parameters which describe the lithospheric and the crustal thinning of the Sardinian passive margin. An excellent fit with present-day basement morphology, Moho geometry, heat flow and gravity anomalies was obtained. They found that the opening of the Tyrrhenian ocean can be adequately described in terms of depth-dependent stretching in an overall 'pure shear' geometry. It was also demonstrated that the lithosphere retained part of its strength during extension: this played a key role in controlling the shape of the basins developed within the rifted margin.

Here, we use this model to analyse in detail the kinematics of extension and, more specifically, the vertical movements which took place during rifting. For this purpose we carry out stratigraphic modelling to quantitatively reconstruct the evolution of the margin (changing depth, morphology of the basin floor, thinning and stretching factors during time). We focus on the vertical movements along the margin which have been so far only qualitatively described.

2. Tectono-stratigraphy of the modelled profile

The 200-km-long modelled section runs in a NW–SE direction from the easternmost parts of Sardinia to the Tyrrhenian abyssal plain (Figs. 1 and 2). To the northwest, the section starts about 20 km from the Sardinian coast. The southestern termina-

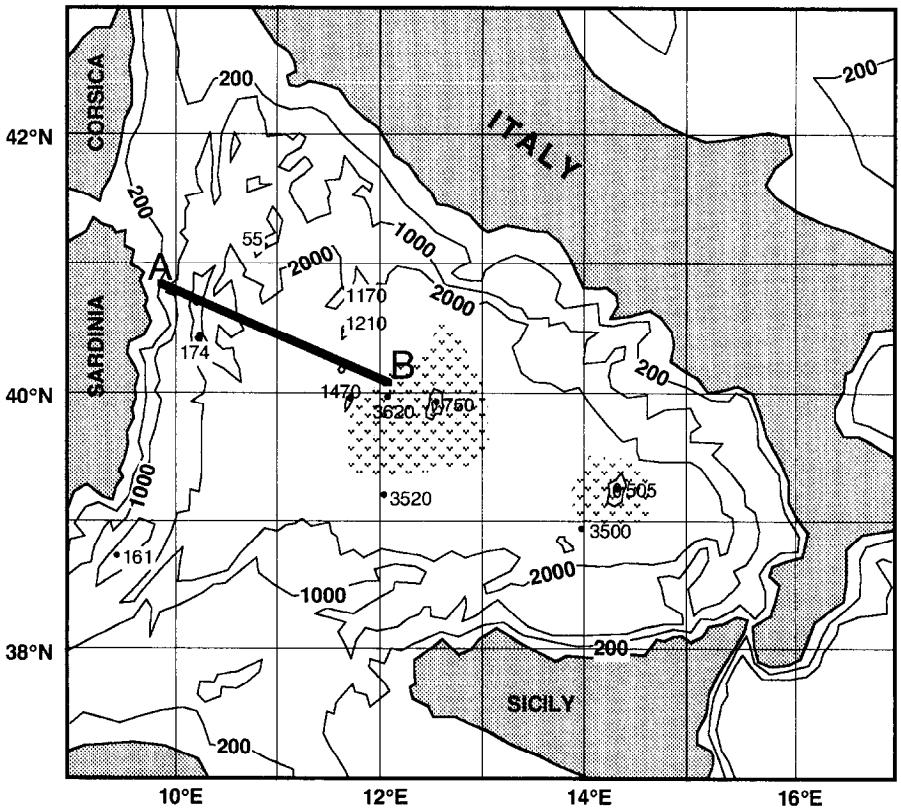

Fig. 1. Simplified bathimetric map of the Tyrrhenian area showing the location of the analysed section. Basaltic areas are also shown.

tion of the profile roughly coincides with the continent–ocean transition. The transect is seismically covered by a number of published profiles (Mascle and Rehault, 1990; Bartole, 1981, and enclosed references) and in particular by the MS-1 seismic profile described by Finetti et al. (1970). Five boreholes (Holes 654, 653, 132, 656, and 652 DSDP/ODP) have been drilled along the transect providing a good calibration and sedimentological characterisation of the sediments. To construct a complete section across the margin we integrated reflection and refraction seismic data with borehole data. We then depth-converted the obtained section using velocities measured in boreholes (Mascle and Rehault, 1990), refraction and multi-channel seismic experiments (Morelli, 1985; Mascle and Rehault, 1990, respectively). The sea-floor along the profile shows a step-wise deepening with a western step at about 1500 m depth, a central one at 2500 m and an abyssal plain which lies at about 3500 m (Fig. 2). The three steps are generally referred to as the upper, middle and lower margin, respectively (Kastens et al., 1988).

The seismic coverage across the upper margin allows for a good control on the geometry of the horizons used in this study, further calibrated with well ODP 654. Some doubts exist on the position of the top Tortonian in the Baronie basin (Fig. 2). In the middle margin, the top Messinian and younger horizons are well constrained by seismic and ODP-DSDP boreholes. For the older part of the succession we have adopted the interpretative thicknesses proposed by Curzi et al. (1980) and Mascle and Rehault (1990). The position of the pre-rift basement was derived from refraction seismic data (Duschenes et al., 1986). In the lower margin, the geometry of the various reflectors is well constrained by numerous seismic sections and boreholes (Mascle and Rehault, 1990).

As the sedimentary successions along the profile and the tectono-stratigraphic evolution of the margin have been qualitatively described in several papers (e.g., Curzi et al., 1980; Kastens et al., 1988; Kastens and Mascle, 1990; Sartori, 1990 and references therein), we will only summarise those aspects which are pertinent to our discussion. To the west of the profile, the uppermost pre-rift units consist of Hercynian metamorphic and igneous rocks (Selli, 1974; Bacini Sedimentari, 1977; Finetti and Del Ben, 1986; Sartori, 1990). The Mesozoic to Paleogene sedimentary cover of the Sardinian block, which is known from other parts of the island is largely missing onshore and possibly along the profile because of Messinian or earlier erosion (Carmignani et al., 1989). To the east, the substratum of the syn-rift succession is formed by the stack of Alpine–Apenninic nappes including the ophiolitic remnants of the Jurassic Ligurian–Piemont ocean closed in Tertiary times (I.G.M., 1980; Sartori, 1986) and, locally, by

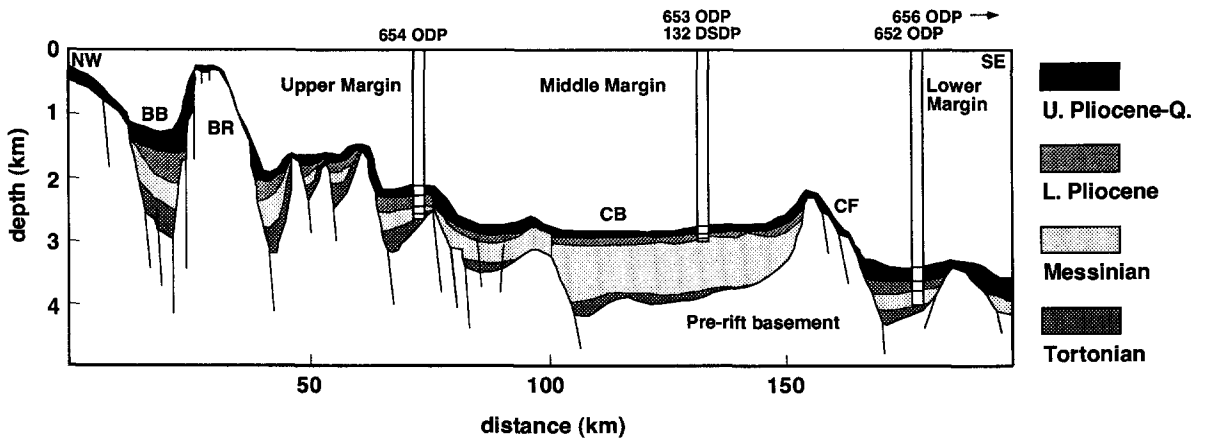

Fig. 2. Section *A–B* (Fig. 1). Observed stratigraphy along the Sardinian passive continental margin. Projections of the ODP and DSDP boreholes are shown. The section is based on Mascle and Rehault (1990), Bartole (1981) and references therein. Time/depth conversion was made according to interval velocities measurements at drilled sites (ODP Leg 107) and to multi-channel seismic profiles information. *BB* = Baronie basin, *BR* = Baronie ridge, *CB* = Cornaglia basin, *CF* = Central Fault.

Alpine metamorphic rocks (Sartori, 1986). The transition between the Hercynian and Alpine pre-rift basements seems to occur across a major NE–SW-trending lineament known as the Selli Line or as the Central Fault (Selli, 1985; Sartori, 1986).

Rifting started in the late Tortonian (9–8 Ma) (Sartori, 1990) and ended in the Late Pliocene (3.4 Ma) (Trincardi and Zitellini, 1987) with the appearance of oceanic crust in the Vavilov basin. Extension is recorded only east of the Sardinian mainland and is well documented by fault-controlled thickness changes, tilted blocks, wedge-shaped sedimentary bodies, detrital cones linked to the activity of normal faults as well as by small sedimentary features such as small-scale debris-flow deposits, micro-faults and chaotic beds, microbreccias, and water-escape structures (e.g., Fabbri et al., 1981; Rehault et al., 1987; Kastens et al., 1988; Mascle and Rehault, 1990). Despite the fact that evidence for extension is found all along the margin throughout the entire rifting stage, the site of most intense deformation was localised and shifted towards the southeast in time: it was located in the upper margin in the late Tortonian, at the middle margin in the Messinian and arrived at the lower margin during the Early Pliocene. There is no evidence for phases of quiescence separating discrete deformation events and we, therefore, assume that the changes occurred in a continuous manner.

The Tortonian part of the syn-rift succession is spatially restricted to grabens and half-grabens where it reaches maximal thicknesses of 300–400 m. The succession starts with local subaerial conglomerates evolving upsection to shallow-water glauconitic sands and to open marine nannofossil oozes (Site 654) (Kastens and Mascle, 1990). Tortonian strata are missing on the structural highs and also in inland Sardinia, possibly as a consequence of Messinian erosion (Carmignani et al., 1989). An earlier onset of erosion with crystalline basement exposed already in Tortonian times is, however, suggested by clay-mineralogy data from site 654 (Chamley et al., 1990). Tortonian beds are locally missing also in the lowermost margin because of Messinian erosion.

During the Messinian, the well known evaporitic sequence was deposited (Curzi et al., 1980). The depocentre of the succession was located in the middle margin where the Cornaglia basin was formed and the most complete evaporitic sequence is found: the lower portion is characterised by salt layers, with the occurrence of diapiric structure, and intercalations of clay and anhydrite; the upper sequence is mainly constituted of alternating gypsum and marls (Curzi et al., 1980). The Messinian sequence, on the structural highs of the upper margin, is characterised by shallow-water carbonates. From the Cornaglia basin, where the thickness is about 800 m, the thickness of Messinian deposits decreases symmetrically toward northwest and southeast (200–300 m). In the lower margin the evaporites are heteropic with clastic deposits interpreted as paleoslope lens (Curzi et al., 1980). Subaerial breccias on the structural highs of the lower margin were detected by Sartori (1990). He also found indications of subaerial environment at ODP Site 656 for the occurrence of red continental paraconglomerates of probable Messinian age. This is compatible with the generalised absence along this segment of the transect of Tortonian beds which has been attributed to Messinian erosion (Mascle and Rehault, 1990).

In the earliest Pliocene, an erosional event, migrating from the lower to the middle margin (Bartole, 1981), caused the formation of a major unconformity at the top of the Messinian evaporites known as the 'M' unconformity (Biscaye et al., 1971). The erosional event was followed by Early Pliocene subsidence of the Tyrrhenian basin. Sedimentological studies (Curzi et al., 1980) constrain the Pliocenic deepening of the Messinian sediments to a value of 1000–1500 m for the upper Sardinian margin and of 2500–3000 for the bathyal plain. The Early Pliocene sedimentation was mainly characterised by nannofossil oozes. The thickness of this unit does not exceed 200–300 m with minimum values on the Cornaglia basin (50–100 m) and is topped by a Middle Pliocene unconformity ('X' of Selli and Fabbri, 1971) which represents the break-up unconformity of the Tyrrhenian Sea (Trincardi and Zitellini, 1987).

During the drifting stage, an up to 400-m-thick succession of Late Pliocene–Pleistocene pelagic calcareous mud, volcanic ashes and sapropel was deposited indicating a general transgressive phase from the end of the Messinian until the present. The maximum thickness of the Late Pliocene–Pleistocene sediments is found in the lower margin (Trin-

cardi and Zitellini, 1987). Towards the northwest the thickness decreases to values between 100 and 200 m at ODP/DSDP Sites 653 and 132 with the exception of the Sardinian basin where it reaches 500 m due to large clastic input from the inland.

3. Modelling of the basin-fill

3.1. Modelling technique

To model the east Sardinia passive margin we used a finite-difference kinematic model (Kooi et al., 1992) in which the analysed transect is subdivided in 40 boxes of 5 km width. For each box we specify a crustal (δ) and a subcrustal (β) thinning factor (Royden and Keen, 1980). Crustal and subcrustal thinning factors are defined as the ratio between the initial and final thickness of the crustal and subcrustal layers, respectively. This has the advantage of facilitating direct comparisons with the stretching factors. Flexural compensation of changing loads has been used in the model incorporating a depth of necking of 25 km (Fig. 3) and an effective elastic thickness defined by the 400°C isotherm (Spadini et al., 1995). Following Braun and Beaumont (1989) we define the depth of necking as the level which experiences no vertical movement in the absence of gravity forces. Basement subsidence is calculated for the adopted thinning factors and corrected for the loading effect of water and/or sediments. The space between the imposed water-depth and the calculated basement position is subsequently filled by sediments. Sediment compaction is taken into account using an exponential porosity–depth relation (Table 1). Other physical parameters used for modelling are given in Table 1.

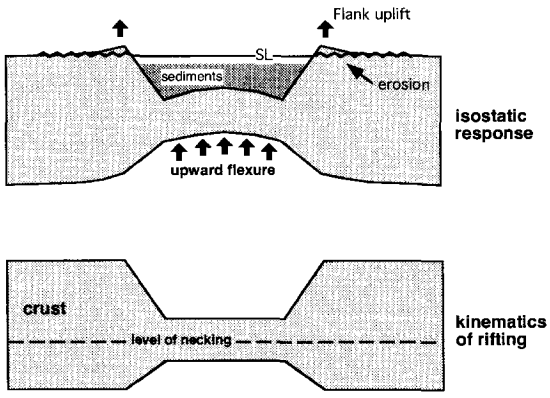

Fig. 3. Schematic representation of the effect of a deep level of necking controlling the thinning of the crust (Kooi et al., 1992): an overall upward state of flexure, deep basin troughs and uplift of the rift flanks are expected. Spadini et al. (1995) constrained the depth of necking for the Tyrrhenian basin at 25 km. This is a very deep value considering that the pre-rift thickness of the Tyrrhenian crust was around 30–35 km.

Table 1
Model parameters

	Value	Definition
a	80 km	initial lithospheric thickness
c	30 km	initial crustal thickness
T_0	0°C	surface temperature
T_a	1333°C	astenosphere temperature
k	7.8×10^{-7} m^2/s	thermal diffusivity
T_e	400°C	isotherm describing EET
α	3.4×10^{-5}°C	thermal expansion coefficient
g	9.8 m/s^2	gravitational acceleration
ρ_c	2800 kg/m^3	surface density crustal rock
ρ_m	3330 kg/m^3	surface density mantle rock
ρ_s	2800 kg/m^3	sediment grain density
ρ_w	1030 kg/m^3	water density
ϕ_0	0.55	sediment surface porosity
c	0.55 km^{-1}	compaction depth constant

3.2. Paleo-water depth

The ODP wells (Kastens and Mascle, 1990) obviously represent the only data points for paleo-water-depth estimates. For the parts of the section between the wells and for the time interval for which no sediments are preserved, no direct estimate is possible. First-guess values were derived by interpolating between the data points and considering the relative vertical position of the different segments as derived from seismic and sedimentological data. With a trial-and-error procedure, these estimates were then varied in order to fit the observed stratigraphy. The resulting water-depth evolution (Fig. 4) is quantitatively coherent and provides an indirect output of the model giving previously unknown information. This is particularly interesting to predict phases of emersion for which no direct record is preserved. Although paleo-water-depth estimates based on sedimentological and paleontological data have uncertainties vary-

ing from 100 m, for the shelf deposits, to 300–400 m for the deeper facies, our results are likely to have a small dependence from the paleo-water depth due to the very short duration of the post-rift phase and the strongly regional compensation of loads adopted in our model.

3.3. Sea-level changes

Our model also includes relative sea-level changes taken from the curves of Haq et al. (1987) which may be partly of eustatic and partly of tectonic origin (Cloetingh, 1991). We introduced a correction for the Messinian time when the Mediterranean was temporally separated from the Atlantic and the Tyrrhenian Sea basin was repeatedly dried out (Cita et al., 1990). The duration of these flooding and evaporation events was shorter than our 2-m.y.-time window and we have, therefore, conventionally adopted a value of −500 m for the average sea-level value during the considered time interval (see discussion below) (Fig. 4).

3.4. Crustal and subcrustal thinning factors

The total thinning factors adopted in the model (Fig. 5) are derived by comparing the present-day crustal and lithospheric thickness for each box with the pre-rift values which are assumed to be constant across the entire future margin and correspond to the present-day thicknesses in the mostly undeformed Sardinia block (30 and 80 km, respectively) (Spadini et al., 1995) (Fig. 5). Using these values for a rifting duration of 6 m.y., between 9 and 3 Ma (Sartori, 1990), the model predicts a correct basement topography but a geometry of the syn-rift succession which is substantially different from the observed stratigraphy (Fig. 6a). A single-step evolution is

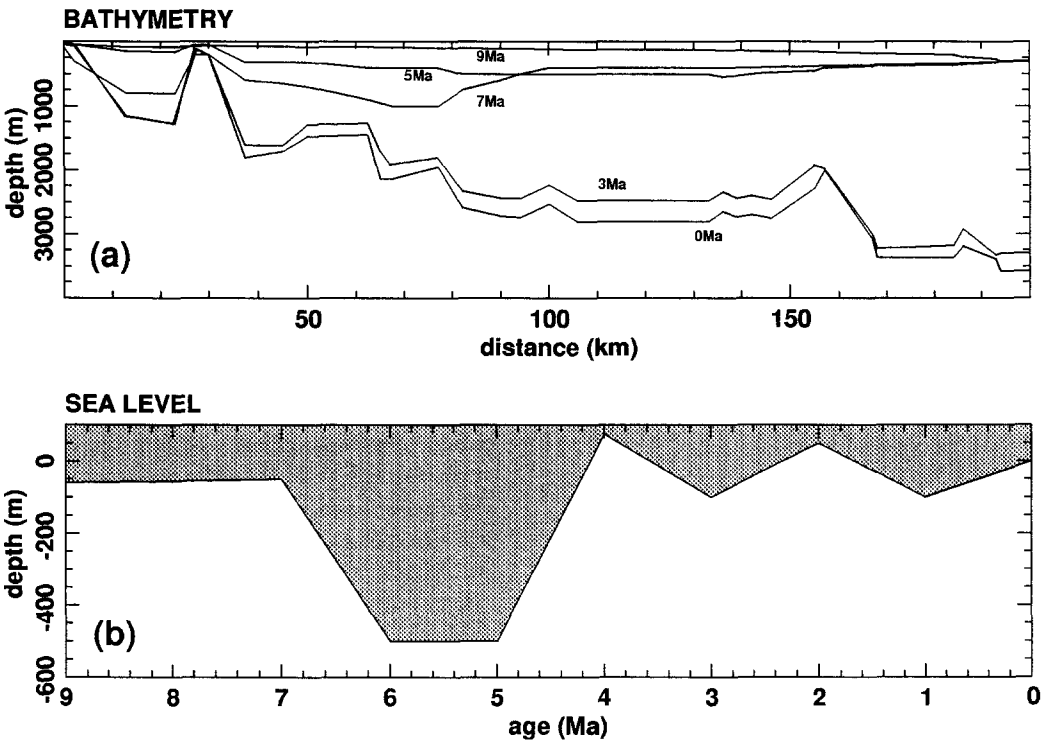

Fig. 4. Paleobathymetric variations predicted by the model for different time interval (a) and sea-level changes used in the modelling (b) (see discussion in the text).

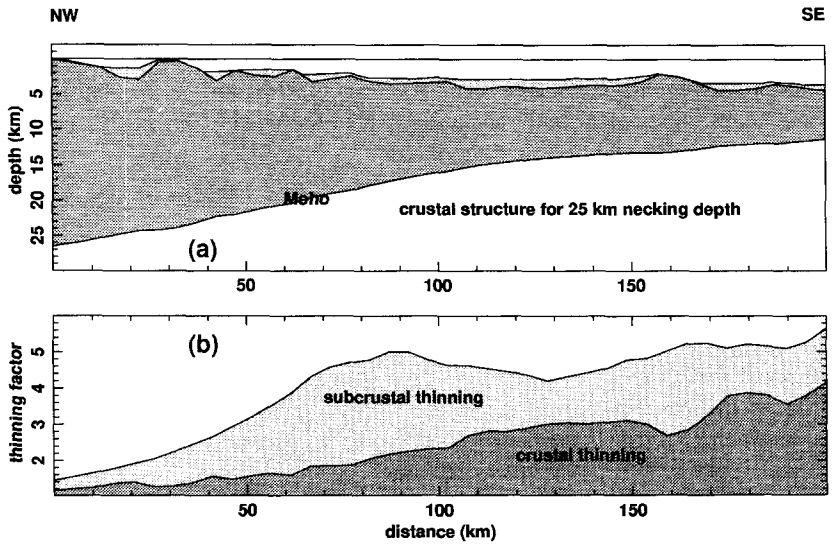

Fig. 5. (a) Predicted crustal geometry from a flexurally compensated model accounting for a depth of necking of 25 km (Spadini et al., 1995). (b) Total crustal and subcrustal thinning factors are derived assuming initial crustal and subcrustal thicknesses of 30 and 80 km, respectively.

further in contradiction with several observations which demonstrate a southeastward shift of the site of extension in time (Kastens and Mascle, 1990; Sartori, 1990). In order to describe these kinematic changes we have subdivided the rifting interval in three continuous steps of 2 m.y. at 7 Ma, 5 Ma and 3 Ma. In our calculation, entire numbers of m.y. are used to define these stages corresponding to the Tortonian, Messinian and Early Pliocene rifting steps; more correct estimates, 6.5 Ma, 4.8 Ma and 3.5 Ma, respectively (Kastens and Mascle, 1990), do not significantly change our results. Since there is no evidence for quiescence phases separating different rifting pulses, these steps are only artificial separations of a continuous process. While the total thinning factors are fixed, the partial ones for the various stages are not. With a trial-and-error procedure they were varied in order to fit the seismic and geological observations, with the constraint that the product of the factors for the single steps must equal the measured thinning factor for that specific box. With this scenario we obtained a good fit with the observed geometries (Fig. 6b). Fig. 7 shows the predicted changes of the thinning factors through time.

4. Quantitative reconstruction of subsidence and basin stratigraphy of the Sardinian margin

4.1. Mode and rate of extension

Similar to many other basins, there is an ongoing debate whether the geometry of lithospheric extension in the Tyrrhenian basin reflects a 'pure shear' or a 'simple shear' configuration (Wang et al., 1989; Rehault et al., 1990; Mascle and Rehault, 1990).

Diagrams of Fig. 7 demonstrate an overall tendency for the site of maximal crustal thinning to coincide with the site of maximal subcrustal thinning. A simple-shear geometry with the site of subcrustal thinning significantly displaced with respect to the crustal one produces a stratigraphic and, more important, a heat-flow pattern different from the observed ones. As further discussed below, our pure-shear geometry produces a remarkable fit with the measured heat flow. This seems to exclude the existence of major low-angle faults cutting through the whole lithosphere and displacing laterally the thinning. The subcrustal thinning factor is generally higher than the crustal one. The difference between the two is largest during the first rifting step, it then

decreases and is practically eliminated during the last time interval before the break-up.

The opening of the Tyrrhenian Sea, therefore, can be described as having a depth-dependent, pure-shear geometry. In the first phases, subcrustal thinning was much stronger than the crustal one, which suggests a heat input in the system larger than that provided by the extension. Since information about the pre-Tortonian sediments is lacking, we do not know the time of the onset of this process which could have started slightly earlier than the onset of crustal thinning. This pattern of heat input preceding or overlapping with the very first stages of rifting has been recognised recently in a number of extensional settings like the Mesozoic passive margin of Adria presently exposed in the Southern Alps (Bertotti and ter Voorde, 1994) and in the North Sea 'triple junction' (Hendrie et al., 1993).

4.2. Rifting stage

In late Tortonian times (between 7 and 9 Ma) extension in the future passive margin first affected the lithospheric segment adjacent to onland Sardinia. Crustal thinning factors compatible with the observed stratigraphic pattern reach maximum values of ca. 1.20 in the segment around 50 and 80 km and gently decrease in a rather symmetric fashion both to

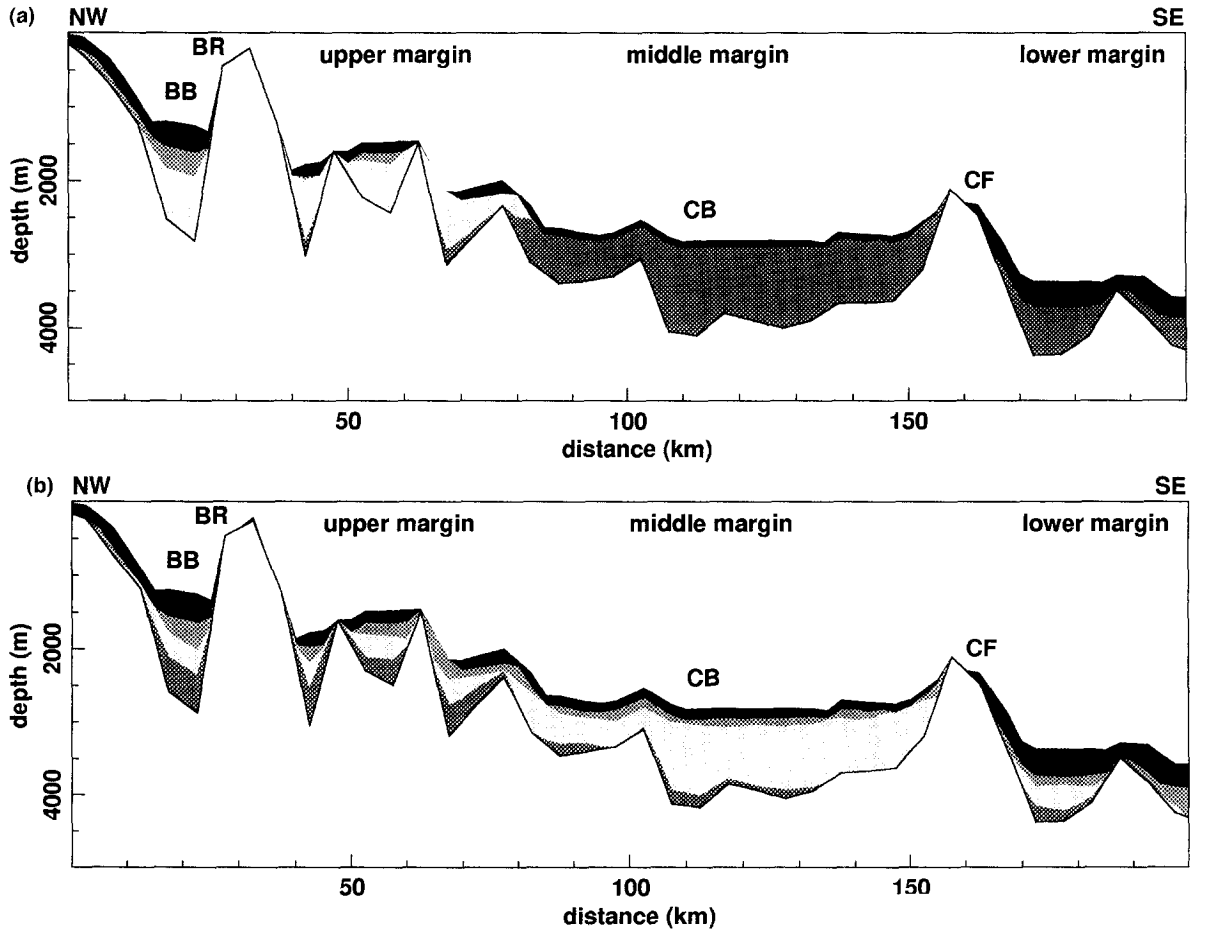

Fig. 6. (a) Predicted stratigraphy for a single rifting event applying the measured thinning factors (Fig. 4) for a rifting duration of 6 m.y. The resulting geometry is substantially different from the observed one (Fig. 2). (b) Basement geometry and stratigraphy predicted by the model incorporating three thinning phases of finite duration. *BB* = Baronie basin, *BR* = Baronie ridge, *CB* = Cornaglia basin, *CF* = Central Fault.

the northwest and to the southeast (Fig. 7). The average crustal thinning factor is 1.12 (Table 2). The subcrustal lithospheric thinning factors (average = 1.5) are much higher than the crustal ones and show a similar pattern across the margin with the highest values found around 70 km southeast of the profile margin (Fig. 7). Subsidence was strongest in the upper margin coinciding with the site of maximum thinning. On the two sides of this segment very limited subsidence took place (Figs. 8 and 9). In onland Sardinia, outside the profile, the model predicts an uplift of about 400 m. Given the suitable climatic conditions this could have caused substantial erosion (Chamley et al., 1990) and at least partly explains the absence of the Mesozoic to Paleogene sedimentary cover in northeastern Sardinia

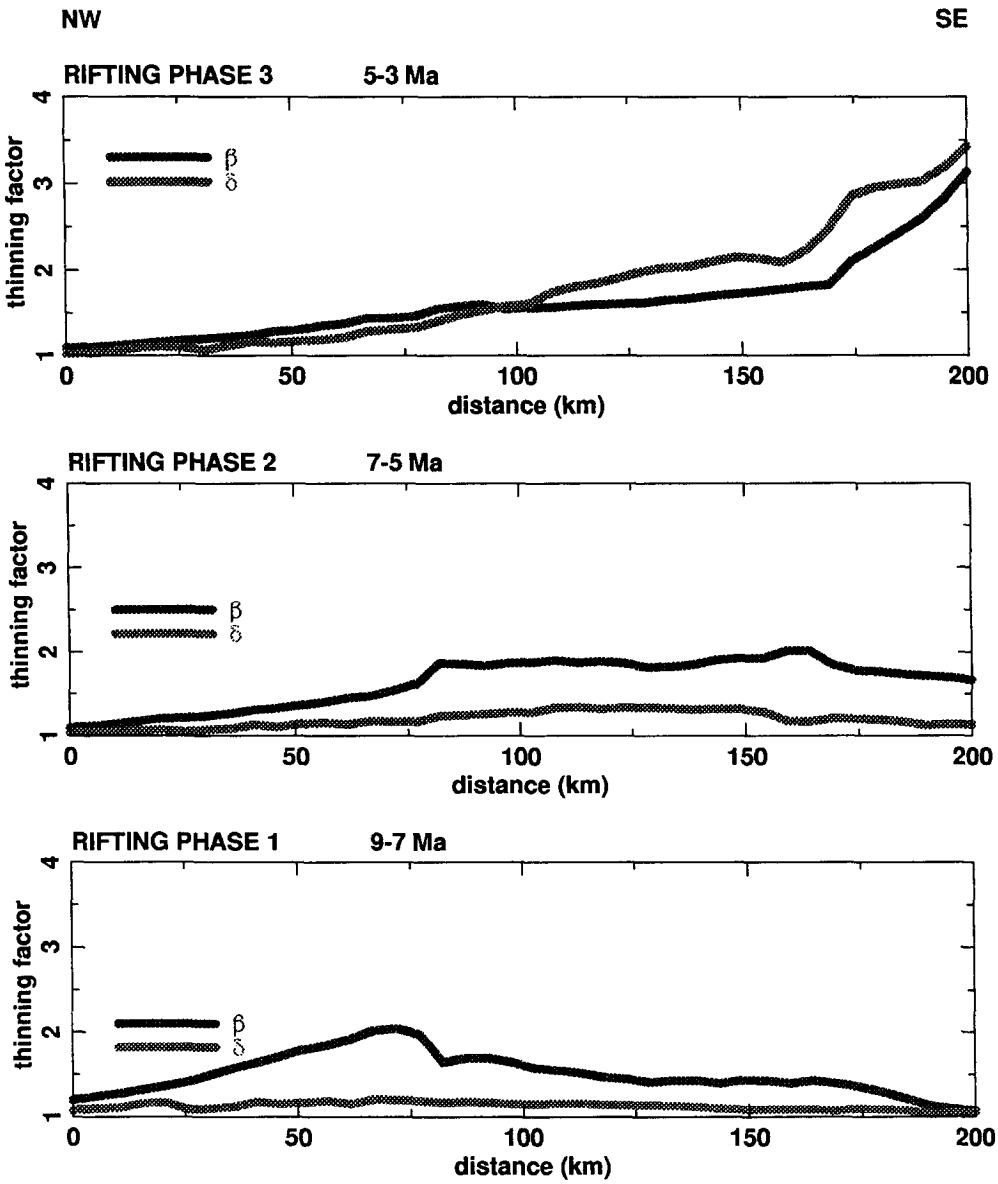

Fig. 7. Subcrustal (β) and crustal (δ) partial thinning factors for the three rifting stages adopted.

(Carmignani et al., 1989). In the upper margin, the basement subsidence was only partly compensated by sedimentation and the basin floor deepened to 800–1000 m in accordance with the transgressive trend detected in the Tortonian deposits (ODP Site 654). The continuity of the basin was interrupted by a prominent morphological high, the Baronie ridge, for which our model predicts a limited emersion above sea-level. Further to the southeast, in the future lower margin, only little sediment was deposited and water depths are of about 300–400 m at the most with large areas emerging above sea-level (Fig. 8).

During the Messinian rifting stage (from 7 to 5 Ma) the site of strongest thinning shifted to the southeast and was located at the middle margin (Fig. 7). Crustal thinning factors for this stage are higher than during the previous step and reach a maximum value of 1.35 at 110–120 km from the northwest end of the profile. The thinning factors then decrease on both sides with a distribution quite symmetrical with respect to the peak values. The average thinning factor across the whole basin is 1.18 (Table 2) for the crust and 1.63 for the subcrustal layer. Subcrustal lithospheric thinning factors (Fig. 7) are still substantially higher than for the previous time step but the ratio between the two is now decreasing. Neglecting the two relative peaks at 80 and 170 km, the thinning factors along the transect show a broad maximum between 90 and 160 km and then symmetrically decreasing values to the sides. The maximum of the subcrustal and crustal thinning factors roughly coincide.

As a response to the thinning factors distribution, the axis of subsidence was located at this stage in the middle margin leading to the formation of the Cornaglia sedimentary basin. The pre-rift basement reached depths of 1000–1200 m below the reference level (present-day sea-level) at 5 Ma (Figs. 8 and 9). Thick sedimentary successions were deposited in this time frame in the Cornaglia basin; the upper morphology of the basin was quite smooth and at 5 Ma was lying approximately 1000 m below the reference level (dashed line in Fig. 8). At the same time, the pre-rift basement of the Central Fault area (site D in Fig. 9) and of the Baronie ridge, at the northwestern end of the profile (Fig. 8), was undergoing slight uplift as a direct consequence of the persisting strength of the Sardinian lithosphere during rifting. The Baronie ridge remained a prominent morphological feature and in times of very low sea-level it must have reached elevations of several hundred metres above the surrounding sea and, possibly, thereby interrupting the connections between the Sardinian continent and Baronie basin from the Cornaglia basin. In the southeastern part of the transect, only limited basement subsidence was taking place (Figs. 8 and 9). The water depths across the whole future margin were highly variable because of the repeated interruption of the connection with the Atlantic Ocean (Cita et al., 1990). Similarly to the other Mediterranean basins, the salinity crises and the desiccation events of the Tyrrhenian basin were repeated at different times, contemporaneous with the Messinian subsidence, allowing for the deposition of thick evaporitic sequences.

During the Early to Middle Pliocene, rifting continued but the site of strongest thinning was located on the lower margin, i.e. close to the site of oceanic crust formation in the Late Pliocene. The highest crustal thinning factors derived from the model reach values up to 3 and are found in a 30–40-km-wide zone at the southeastern end of the profile (Fig. 7). However, thinning was by no means confined to this

Table 2
Crustal thinning factors

Phase	Time interval (Ma)	Mean δ u. margin	Mean δ m. margin	Mean δ l. margin	Mean δ	Cumulative δ
3	5–3	1.14	1.81	**2.89**	1.95	2.57
2	7–5	1.10	**1.29**	1.17	1.18	1.32
1	9–7	**1.15**	1.14	1.07	1.12	1.12

zone and must have affected also the middle margin. The average crustal thinning is at this stage about 1.95, i.e. substantially higher than the previous ones. Similarly to the crustal ones, the subcrustal lithospheric thinning factors (average = 1.64) show the highest values in correspondence to the future continent–ocean transition (Fig. 7). Continuing a trend already seen for the previous time step, the difference between the two factors for each box is further reduced and they practically coincide. A high heat flow associated with strong lithospheric thinning is reflected in the downward increase of automorphic chlorite at the expense of smectite and kaolinite observed at Site 652 (Chamley et al., 1990).

Subsidence of the order of a few hundred metres is predicted for the upper margin where the Baronie ridge remained a prominent morphological feature, but at 5 Ma was already below sea-level (Figs. 8 and 9). The lower and, to a lesser extent, the middle margin were clearly subsiding and, at the end of rifting, the pre-rift basement of the middle to lower margin was located at ca. 3800–4000 m below the present-day sea-level. In contrast with the previous time steps, the areas flanking the site of maximum extension, also underwent subsidence. This is possibly a consequence of the very strong lithospheric thinning which dramatically heated the lithosphere and thereby caused a decrease of its effective elastic thickness (from 15–20 km in the Messinian to 10 km in the Early Pliocene, with a minimum of 5 km in the lower margin; Spadini et al., 1995). Sedimentation did not keep pace with the basement subsidence and the basin floor substantially deepened. This was obviously particularly relevant for the lower margin

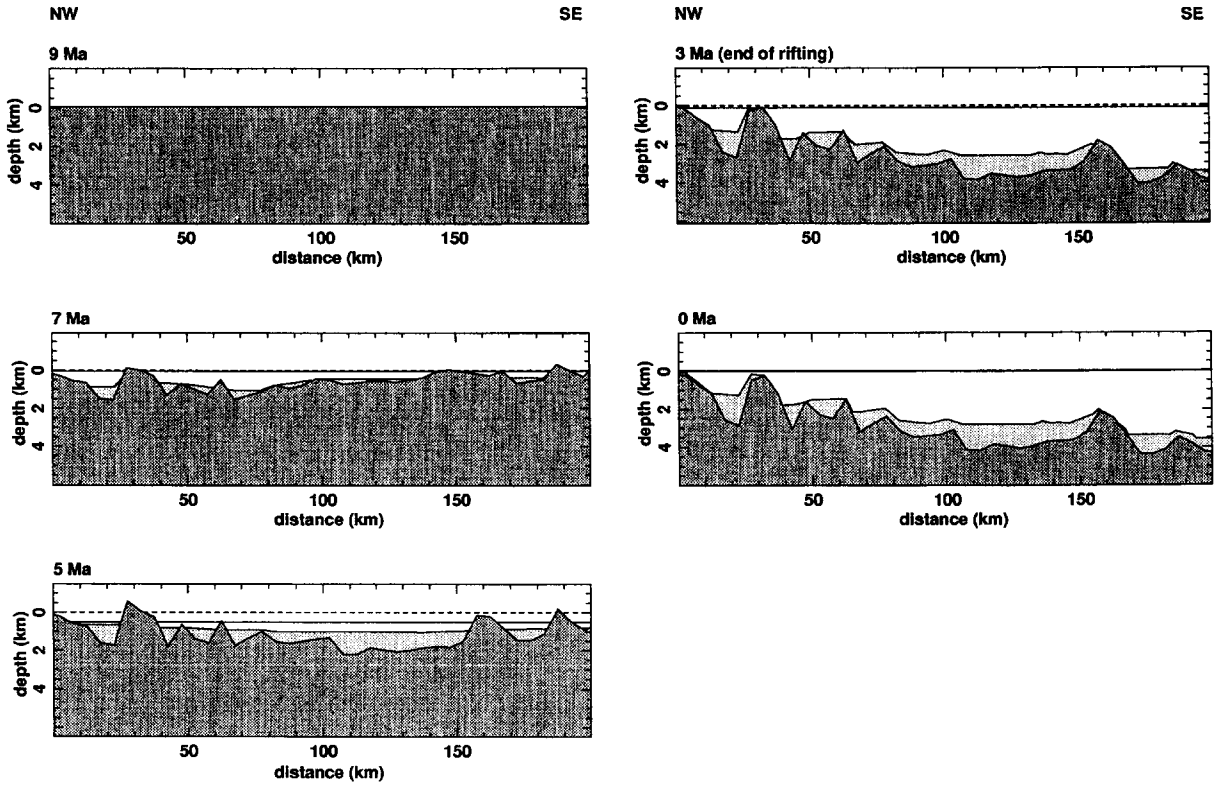

Fig. 8. Basement and basin topography for different time slices of the modelled evolution. Dashed line is the reference for the present-day sea-level; dark grey = pre-rift basement; light grey = syn-rift and post-rift sedimentary sequences.

where the water–sediment interface moved from a depth of ca. 800 m at 5 Ma to about 3000 m 2 m.y. later.

4.3. Post-rift stage

At the end of rifting, the morphology of the margin was quite similar to the present-day situation followed by basinwide deepening during the post-rift phase (Fig. 8). The model predicts a basement subsidence of up to 500 m for the lower margin, with lesser values for the middle and upper parts of the margin. The deposition of the thin Upper Pliocene–Quaternary sequence implies an increase in water depths not larger than 200–300 m.

We are aware of the fact that this is in contrast to some analyses of benthic foraminifera which suggest a deepening of the margin from 1500 m (ODP Site 654) to 2500 m (ODP Site 652) for the last three million years (Hasegawa et al., 1990). However, the post-rift subsidence estimate given by the model is very robust and even assuming a break-up at 4 Ma, and thereby increasing by 25% the post-rift duration, the deepening is no more than 500 m (Fig. 10).

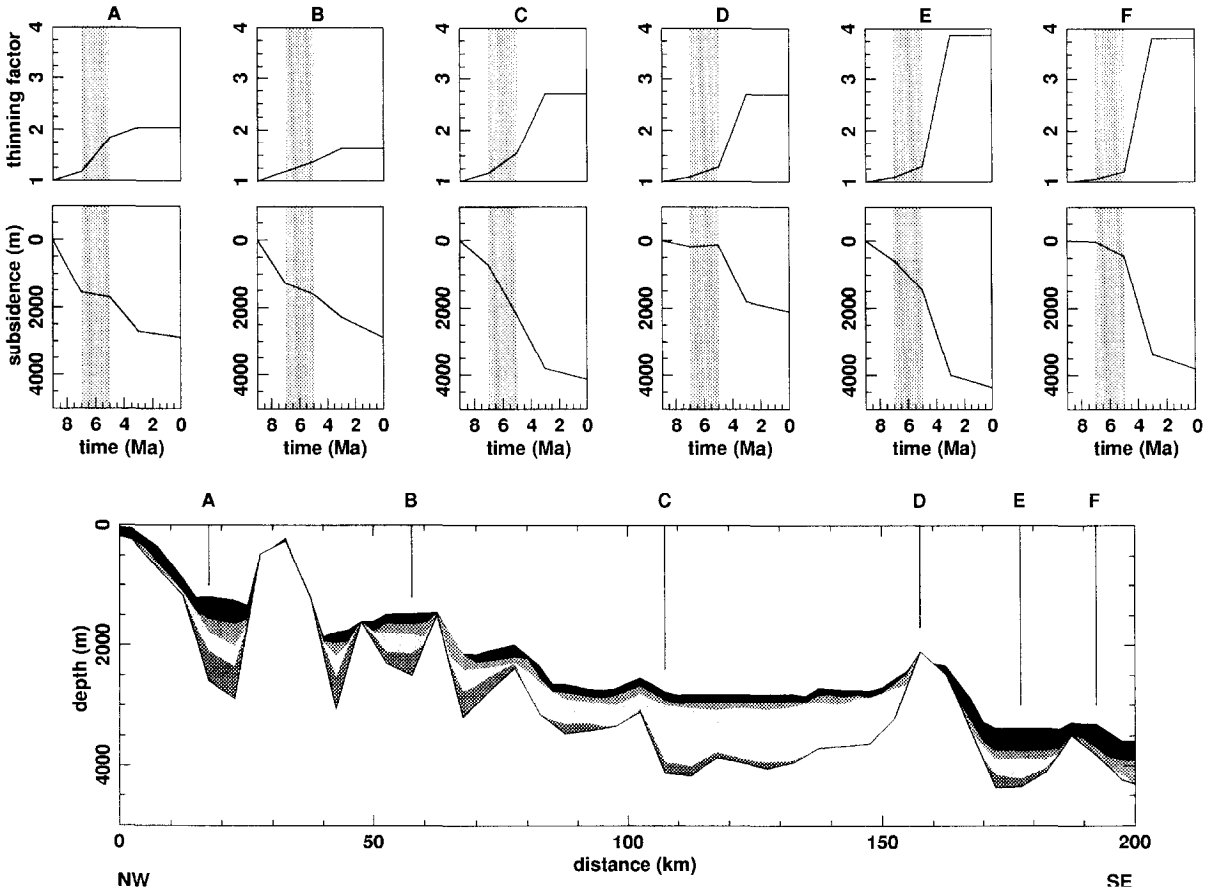

Fig. 9. Subsidence patterns for different locations along the analysed transect. Crustal thinning factors versus time are also shown for the same sites. Note that slowing down of subsidence (sites *A*, *B*) and uplift trends (site *D*) are predicted for a time interval (7–5 Ma) characterised by acceleration of thinning (indicated by shaded bars). The apparent paradox can be explained taking into account the flank uplift flexural effect (see discussion in the text).

5. Basin depth before and after the Messinian salinity crisis

DSDP Leg 13 and ODP Leg 107, supplemented by more than twenty years of seismic investigations, demonstrated that large parts of the Tyrrhenian basin floor are underlain by an up to 900-m-thick sequence of evaporites of Messinian age interpreted by Hsü et al. (1973) as shallow-water sediments deposited in basins lying at least 2 km below the level of the Atlantic prior to the onset of the salinity crisis. This gave rise to a long-standing debate mostly concerning the sedimentary processes which led to the deposition of the evaporites, and the configuration of the basin immediately before and after the salinity crisis (e.g., Cita, 1991). While there seems to be a general consensus that the evaporites were deposited under shallow-water conditions, this does not appear to be the case for the depth of the basin floor with respect to the surrounding areas. According to Ryan and Cita (1978), the western and eastern Mediterranean immediately before the onset of the Messinian crisis were at a depth of few kilometres below the surrounding continental areas. Admittedly, "the most compelling arguments for postulating deep Mediterranean basins were the awareness the bimodal depth distribution between continents and oceans, and the appreciation the depth of the oceanic crust is related to its age" (Ryan and Cita, 1978, p. 194). While this line of reasoning is correct for most of the Mediterranean basins, it cannot hold for the Tyrrhenian basin which during the Messinian was still underlain by continental crust.

Our numerical model provides constraints on the position of the basement and of top of the sediments with respect to the present-day reference level, roughly corresponding to the surrounding continental areas. This gives an estimate of the maximum height of the water column that must have repeatedly evaporated in order to form the evaporitic sequence. Provided that rifting was the main tectonic process which led to the formation of the Tyrrhenian oceanic crust throughout the history of the rifted margin, the depths of the top of the pre-rift basement and, therefore, of the top of the syn-rift succession can vary only within a limited range of values. At 7 Ma, i.e., immediately before the onset of the Messinian salinity crisis, the western part of the Tyrrhenian basin covered by our profile was characterised by a trough located a few tens of kilometres southeast of onland Sardinia with the top of pre-Messinian succession lying ca. 1 km below the present-day sea-level. The basin floor was rapidly shallowing towards the northwest and, more gently, towards the southeast, reaching depths of a few hundred metres (Fig. 8). In the southeasternmost 60 km of the profile, large

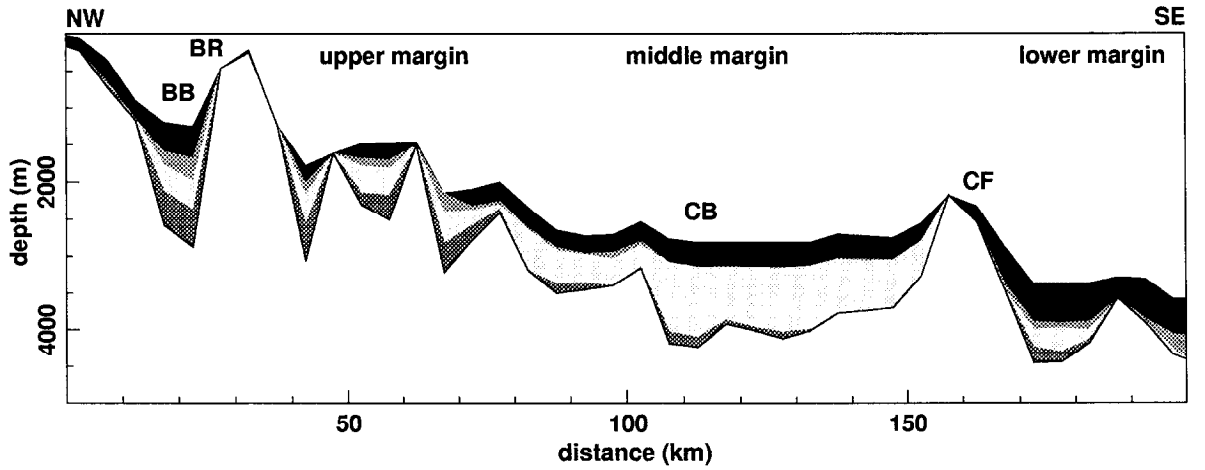

Fig. 10. Predicted stratigraphy for a 4-Ma post-rift phase. Post-rift sedimentary unit in black. Considering a longer post-rift phase (break-up at 4 Ma) we obtain a surplus of post-rift sediments in comparison to the observed record (Fig. 2). In order to obtain a good fit with the observed stratigraphy the water depth at the end of rifting can be decreased: in this case the predicted deepening of the basin during the post-rift phase reaches values around 400–500 m. *BB* = Baronie basin, *BR* = Baronie ridge, *CB* = Cornaglia basin, *CF* = Central Fault.

areas were above the reference level. At 5 Ma, that is after the end of the salinity crisis, the morphology of the basin changed quite drastically resulting in a much more regular shape. With the exception of the Baronie ridge to the northwest and of two prominent highs in the southeast, most of the top of the Messinian sequence was lying approximately 1000 m below the reference level. The Baronie basin, at the northwest end of the profile, was at a depth of ca. 700 m below the same level (Fig. 8). Our numerical model, therefore, predicts a sediment–water interface quite stable in elevation from 7 to 5 Ma, usually lying up to 1000 m below the present-day sea-level. Accepting the estimates given by Ryan and Cita (1978) of > 2 km for the depths of the Balearic ocean and for the Eastern Mediterranean, we conclude that the Tyrrhenian basin floor, during the Messinian, was lying at least 1 km higher than the surrounding Mediterranean basins. To cross-check this conclusion, we modelled the heat-flow pattern predicted for a scenario where the basin floor reached a depth of more than 2000 m at the beginning of the salinity crisis. To achieve this, we concentrate the entire lithospheric thinning and the basement subsidence of the Tyrrhenian during the Tortonian, the model can accomplish for a Messinian sea-level fluctuation of > 2000 m. The heat-flow at 0 Ma for such a scenario (Fig. 11) shows a misfit of about 20 mW/m^2 between the predicted values and the observed one. A strong thinning phase during the Early Pliocene (Fig. 7) as adopted in our model predicts, conversely, a heat-flow signature in a very good agreement with the observations (Fig. 11). We conclude therefore that the substantial deepening of the basin floor occurred after the end of the salinity crisis beginning with the earliest Pliocene. After 5 Ma, with the concentration of extension in the lower margin, strong subsidence affected the already thinned continental crust of the Tyrrhenian basin and the whole margin approached the present-day depths.

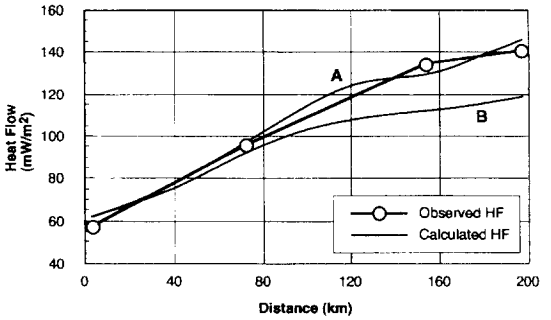

Fig. 11. Predicted heat-flow trends across the margin for two different scenarios of lithospheric thinning. $A = 6$ m.y. of rifting with a strong Early Pliocene thinning event concentrated in the lower margin (Fig. 6); this produced the tectonic evolution shown in Fig. 7; B = concentration of lithospheric thinning during the Tortonian, producing a deep basin before the Messinian desiccation event (2000 m of sea-level fluctuation). Comparison with the observed heat-flow trend (Hutchinson et al., 1985) is also shown. See text for discussion.

6. Conclusions

The east Sardinia margin, like many other rifted margins, is characterised by a complex subsidence pattern changing through time. At one time step, different segments of the future margin were undergoing vertical movements differing in absolute value and, possibly, even in sign (Fig. 9). The general pattern of the Sardinia margin for a given time interval was given by a few tens of kilometres wide zone of strong thinning and subsidence, flanked by areas which, despite the ongoing thinning, experienced much more limited subsidence or even uplift. This pattern is evident for the Messinian when the flank uplift, located at both sides of the Cornaglia basin, is not obliterated by a strong thinning-related subsidence (shaded bar of Fig. 9). The modelling shows that these differing movements are not fortuitous but are both expression of the same rifting process affecting a lithosphere which preserved part of its strength during extension. As a consequence, a dynamic link between the various segments of the margin is established and changing loads are compensated in a regional fashion. Because of the deep depth of necking (Spadini et al., 1995), the regions to the sides of the most strongly thinning regions experience more limited subsidence or even uplift. This has obviously profound consequences on the shape of the sedimentary bodies deposited. Flexural uplift, as a result of lithospheric necking, was proposed for vertical motion at rift flanks by Braun and Beaumont (1989) and Weissel and Karner (1989). Our analysis highlights the importance of this phenomenon within the basin: if the rifting is di-

achronous, i.e., the site of maximum thinning is migrating, the flank uplift is also migrating and these effects are superimposed on the overall subsidence of the margin.

Acknowledgements

We would like to thank R. Sartori and V. Picotti for their help and interest. We also thank C. Banks, Z. Ben-Avraham and B. D'Argenio for careful reviews. This work was funded by the IBS (Integrated Basin Studies) project, part of the Joule II research programme funded by the Commission of the European Communities (contract Nr. JOU2-CT 92-0110). G.B. acknowledges financial support from AWON (project Nr. 751.356.026A). Publication 950324 of the Netherlands Research School of Sedimentary Geology.

References

Bacini Sedimentari, 1977. Sedimenti e struttura del Bacino della Sardegna. Ateneo Parmense, 13: 549–570.

Bartole, R., 1981. Seismic evidence of an earlier Pliocene erosional surface in the deep part of the Tyrrhenian Sea. In: F.C. Wezel (Editor), Sedimentary Basins of Mediterranean Margin. Tecnoprint, Bologna, pp. 127–145.

Bertotti, G. and ter Voorde, M., 1994. Thermal effects of normal faulting during rifted basin formation, 2. The Lugano–Val Grande normal fault and the role of the pre-existing thermal anomalies. Tectonophysics, 240: 145–157.

Biscaye, P., Ryan, W.B.F. and Wezel, F.C., 1971. Age and nature of the Pan-Mediterranean subbottom reflector M. In: D.J. Stanley (Editor), The Mediterranean Sea: A Natural Sedimentation Laboratory. Dowden, Hutchinson and Ross, London, pp. 83–90.

Braun, J. and Beaumont, C., 1989. A physical explanation of the relation between flank uplifts and the breakup unconformity at rifted continental margins. Geology, 17: 760–764.

Carmignani, L., Cherchi, A. and Ricci, C.A., 1989. Basement structure and Mesozoic–Cenozoic evolution of Sardinia. In: A. Boriani, M. Bonafede, G.B. Piccardo and G.B. Vai (Editors), The Lithosphere in Italy. Accademia Nazionale dei Lincei, Roma, pp. 63–92.

Chamley, H., Debrabant, P., Robert, C., Mascle, G., Rehault, J.P. and Aprahamian, J., 1990. Mineralogical and geochemical investigations on latest Miocene deposits in the Tyrrhenian Sea (ODP Leg 107). Proc. ODP, Sci. Results, 107: 153–167.

Cita, M.B., 1991. Development of a scientific controversy. In: D.W. Muller, J.A. McKenzie and H. Weissert (Editors), Controversies in Modern Geology. Academic Press, London, pp. 13–23.

Cita, M.B., Santambrogio, S., Mellillo, B. and Rogate, F., 1990. Messinian paleoenvironments: new evidence from the Tyrrhenian Sea (ODP Leg 107). Proc. ODP, Sci. Results, 107: 211–227.

Cloetingh, S., 1991, Tectonics and eustasy: a controversy? In: D.W. Muller, J.A. McKenzie and H. Weissert, (Editors), Controversies in Modern Geology. Academic Press, London, pp. 249–277.

Curzi, P., Fabbri, A. and Nanni, T., 1980. The Messinian evaporitic event in the Sardinia Basin area (Tyrrhenian Sea). Mar. Geol., 34: 157–170.

Dewey, J.F., Helman, M.L., Turco, E., Hutton, D.H.V. and Knott, S.D., 1989. Kinematics of the western Mediterranean. In: M.P. Coward, D. Dietrich and R.G. Park (Editors), Alpine Tectonics. Geol. Soc. London, Spec. Publ., 45: 265–28.

Duschenes, J., Sinha, M.C. and Louden, K.E., 1986. A seismic refraction experiment in the Tyrrhenian Sea. Geophys. J.R. Astron. Soc., 85: 139–160.

Fabbri, A., Gallignani, P. and Zitellini, N., 1981. Geologic evolution of the peri-Tyrrhenian sedimentary basins. In: F.C. Wezel (Editor), Sedimentary Basins of Mediterranean Margin. Tecnoprint, Bologna, pp. 101–126.

Finetti, I. and Del Ben, A., 1986. Geophysical study of the Tyrrhenian opening. Boll. Geofis. Teor. Appl., 28: 75–155.

Finetti, I., Morelli, C. and Zarudzki, E., 1970. Reflection seismic study of the Tyrrhenian Sea. Boll. Geofis. Teor. Appl., 12, 311 pp.

Haq, B.U., Hardenbol, J. and Vail, P.R., 1987. Chronology of the fluctuating sea-levels since the Triassic (250 my to present). Science, 235: 1156–1167.

Hasegawa, S., Sprovieri, R. and Poluzzi, A., 1990. Quantitative analysis of benthic foraminiferal assemblages from Plio–Pleistocene sequences in the Tyrrhenian Sea, ODP Leg 107. Proc. ODP, Sci. Results, 107: 461–478.

Hendrie, D.B., Kusznir, N.J. and Hunter, R.H., 1993. Jurassic extension estimate for the North Sea 'triple junction' from flexural backstripping: implications for decompression melting models. Earth Planet. Sci. Lett., 116: 113–127.

Hsü, K.J., Ryan, W.B.F. and Cita, M.B., 1973. Late Miocene desiccation of the Mediterranean. Nature, 242: 240–244.

Hutchinson, I., Von Herzen, R.P., Louden, K.E., Sclater, J.G. and Jemsek, J., 1985. Heat-flow in the Balearic and Tyrrhenian Basins, Western Mediterranean. J. Geophys. Res., 90: 685–70.

I.G.M., 1980. Ricerca interprogetto sull'origine ed evoluzione del Mar Tirreno e dei suoi margini. Rapp. Tec. I.G.M., 10, 26 pp.

Kastens, K. and Mascle, J., 1990. The geological evolution of the Tyrrhenian Sea: an introduction to the scientific results of ODP Leg 107. Proc. ODP, Sci. Results, 107: 3–26.

Kastens, K., Mascle, J. et al., 1988. ODP Leg 107 in the Tyrrhenian Sea: insights into passive margin and back-arc basin evolution. Geol. Soc. Am. Bull., 100: 1140–1156.

Kooi, H., Cloetingh, S. and Burrus, J., 1992. Lithospheric necking and regional isostasy at extensional basins, 1. Subsidence and gravity modelling with an application to the Gulf of Lions Margins (SE France). J. Geophys. Res., 97: 17,553–17,571.

Leg 107 Shipboard Party, 1986. A microcosm of ocean basin evolution in the Mediterranean. Nature, 321: 383–400.

Mascle, J. and Rehault, J.P., 1990. A revised seismic stratigraphy of the Tyrrhenian Sea: implications for the basin evolutions. Proc. ODP, Sci. Results, 107: 617–63.

Morelli C., 1985. Geophysical contribution to knowledge of the Mediterranean crust. In: D.J. Stanley and F.C. Wezel (Editors), Geological Evolution of the Mediterranean Basin. Springer-Verlag, New York, pp. 65–82.

Patacca, E., Sartori, R. and Scandone, P., 1990. Tyrrhenian Basin and Apenninic Arc: kinematic relations since late Tortonian times. Mem. Soc. Geol. Ital., 45: 425–451.

Rehault, J.P., Moussat, E. and Fabbri, A., 1987. Structural evolution of the Tyrrhenian back-arc basin. Mar. Geol., 74: 123–150.

Rehault, J.P., Tisseau, C., Brunet, M.F. and Louden, K.E., 1990. Subsidence analysis on the Sardinian margin and the central Tyrrhenian Basin: thermal modelling and heat flow control; deep structure implications. J. Geodyn., 12: 269–310.

Royden, L. and Keen, C.E., 1980. Rifting process and thermal evolution of the continental margin of eastern Canada determined from subsidence curves. Earth Planet. Sci. Lett., 51: 343–351.

Ryan, W.B.F and Cita, M.B., 1978. The nature and distribution of Messinian erosional surface-indicators of a several-kilometer-deep Mediterranean in the Miocene. Mar. Geol., 27: 193–230.

Sartori, R., 1986. Notes on the geology of the acoustic basement in the Tyrrhenian Sea. Mem. Soc. Geol. Ital., 36: 99–108.

Sartori, R., 1990. The main results of ODP Leg 107 in the frame of Neogene to recent geology of perityrrhenian areas. Proc. ODP, Sci. Results, 107: 715–730.

Selli, R. and Fabbri, A., 1971. Tyrrhenian: a Pliocene deepsea. Accad. Nazl. Lincei, Rend. Cl. Sci. Fis., Mat. Nat., 8: 104–116.

Selli, R., 1974. Appunti sulla geologia del Mar Tirreno. In: Paleogeografia del Terziario nell'ambito del Mediterraneo Occidentale. Sem. Fac. Sci. Univ. Cagliari, 43: 327–351.

Selli, R., 1985. Tectonic evolution of the Tyrrhenian Sea. In: D.J. Stanley and F.C. Wezel (Editors), Geological Evolution of the Mediterranean Basin. Springer-Verlag, New York, pp. 131–151.

Spadini, G., Cloetingh, S. and Bertotti, G., 1995. Thermo-mechanical modelling of the Tyrrhenian Sea: lithospheric necking and kinematics of rifting. Tectonics, 14: 629–644.

Trincardi, F. and Zitellini, N., 1987. The rifting of the Tyrrhenian Basin. Geo-Mar. Lett., 7: 1–6.

Wang, C.Y., Hwang, W.T., and Shi, Y., 1989. Thermal evolution of a rift basin: the Tyrrhenian Sea. J. Geophys. Res., 94: 3991–4006.

Weissel, J.K. and Karner, G.D., 1989. Flexural uplift of rift flanks due to mechanical unloading of the lithosphere during extension. J. Geophys. Res., 94: 13,919–13,950.